2024 IEEE/RSJ International Conference on Intelligent Robots and Systems (IROS)
October 14-18, 2024. Abu Dhabi, UAE

Versatile Variable-Stiffness Scooping End-Effector: Tilting-Scooping-Transfer Mechanism for Objects with Various Properties

Yuta TAKAHASHI, Kenjiro TADAKUMA, Kazuki ABE,
Masahiro WATANABE, Shoya SHIMIZU, Satoshi TADOKORO, Tohoku University

***Abstract*—To address the setup and changeover time issues in high-mix, low-volume production systems, we developed an end-effector capable of uniformly scooping, holding, and transporting a wide variety of objects, and demonstrated this system with prototype. Our experiments showed that the prototype was successful in scooping up and transporting a wide variety of objects and could be applied to high-mix low-volume production systems. In addition, the load testing of the spatula and modeling of objects that can be tilted backwards provided insight into further improvements of the scooping performance of this mechanism.**

Keywords— Mechanism Design, Grippers and Other End-Effectors

I. Introduction

A. Research Background

Most of Japan's machinery industry is based on high-mix, low-volume production systems, also known as made-to-order manufacturing. One of the limitations of such systems is the large amount of setup and changeover work required for automation, such as the re-setting of the gripping of a robot arm for each object and replacing the end-effector. Therefore, the demand is high for grippers that can uniformly grasp and transport a wide variety of objects.

Examples of conventional multi-purpose robotic hands include the DLR-hand II [1-2], Bullet-hand [3-4], FRH-4-hand [5], Pisa-IIT-hand [6-7], Soft-hand Pro-D [8], ISR-soft-hand [9], UC-soft-hand [10], and Kanazawa-hand [11]. These multi-fingered robot hands imitate the human hand and are mainly specialized in wrapping and precise grasping tasks.

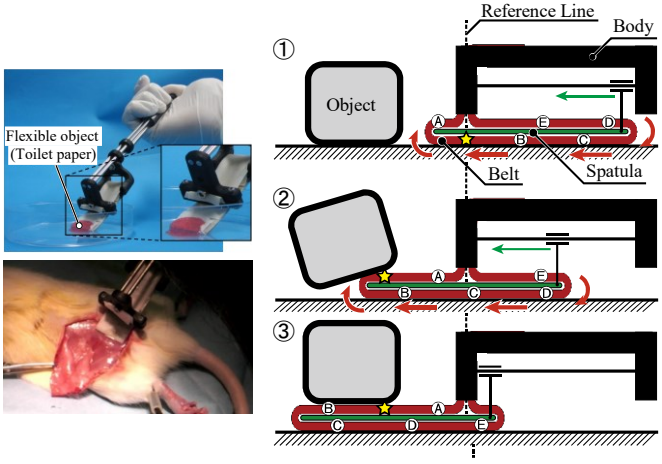

(a) Spatula mechanism for cell sheets; (b) Principle of tip-folding belt
Figure 1. Tip-folding belt mechanism

Figure 2. Prototype shown scooping and carrying a 500-mL PET bottle filled with water

However, it remains difficult to grasp flexible objects, particularly those prone to plastic deformation, owing to the need to apply strong pressure to grasp such objects.

As a solution to this problem, we developed a method of scooping up and transporting objects by inserting a spatula into the gap between the object and its ground surface and using the spatula as a tray. This method is based on the premise that any object on a table or other surface is at least stiff enough to support its own weight. As a reverse version of tablecloth pulling, a spatula can be slid into the gap between an object and the underlying surface, and the spatula can be used as a tray to carry the object. This method does not require the application of any gripping force to an object.

B. Spatula Mechanism for Cell Sheets

We previously introduced a spatula mechanism for cell sheets as a fundamental scooping mechanism [12]. This mechanism enables the manual scooping of extremely flexible, thin, and easily torn objects such as cell sheets. Other mechanisms proposed in previous studies include a gripper with a variable grasping mode developed by Watanabe et al. [13], a parallel flexible gripper developed by Yoshimi et al. [14], an underdriven hand that imitates human picking-up motion [15-16], and a gripper using sliding sheets [17-18].

Fig. 1 illustrates the principle of the investigated tip-folding belt. The belt is fixed to the main body, and the spatula moves back and forth by an advancing/retracting mechanism. The belt moves around the thin plate as the advance/retraction mechanism moves back and forth. Contact of the belt with the object suppresses sliding friction on the object, allowing the smooth insertion of the spatula. The object is then scooped up, held without deformation, and transferred to another location.

The results of this research were obtained via a project funded by the New Energy and Industrial Technology Development Organization (NEDO) (JPNP20016).
Kenjiro Tadakuma, Kazuki Abe, Masahiro Watanabe are with the Graduate School of Engineering Science, Osaka University. Yuta Takahashi, , Shoya Shimizu, and Satoshi Tadokoro are with the Graduate School of Information Sciences, Tohoku University, Osaka University, Japan (*Corresponding author: Kenjiro Tadakuma (email: kenjiro.tadakuma.es@osaka-u.ac.jp)).

The previously published mechanism described above is most suitable for small or thin objects, and it is not versatile. The spatula mechanism for cell sheets has a low load capacity and cannot be used to lift heavy objects.

C. Research Purpose and Paper Structure

In this study, we focused on achieving a versatile end-effector. We designed and realized a mechanism that enables the scooping, holding, and transportation of objects of different shapes, softness, and weights via the same operation.

The remainder of this paper is organized as follows. Section II describes the proposed basic principles of the backward - tilting gap-generation mechanism. Section III describes the design of a prototype integrating the belted tip-folding and stiffness-changing spatula and backward-tilting mechanism, and describes its mode of operation. Section IV describes the experiments conducted using the prototype. Section V describes the modeling and verification of an object capable of backward tilting. Section VI summarizes the results and concludes the paper.

II. Basic Principle of the Backward-Tilting Gap-Generation Mechanism

In addition to heavy objects, the spatula mechanism for cell sheets requires a gap to insert the spatula, as shown in Fig.3(a). Therefore, it is difficult to scoop up objects for which the bottom contour forms an angle of ≥ 90° relative to the floor. As shown in Fig. 3(b), it is theoretically impossible to insert the spatula, because of the absence of a gap. As a solution to this problem, we have developed a "backward-tilting gap-generator for spatula insertion" which generates a gap wide enough to allow the insertion of a spatula by tilting the object backwards. This is inspired by "kuzushi," a technique used in judo to break an opponent's posture.

This section describes the basic principle of the gap-generation mechanism for backward-tilting spatula insertion. In this study, the left-hand side of the plane was treated as the backwards direction and the right-hand side as the forward direction, as shown in Fig. 4.

First, a pivot was placed in contact with the lower left-hand edge of the object, and the point was the center of rotation. Contact was made from the position of the maximum moment,

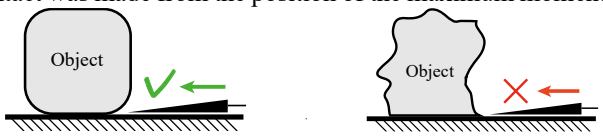

(a) Object under which the spatula is easy to insert.

(b) Object under which the spatula is difficult to insert.

Figure 3. Scooping ability depending on the features of the object base

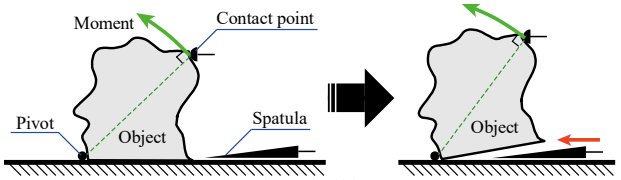

Figure 4. Principle of Backward Tilting Gap Generation Mechanism

and a force was generated in the direction perpendicular to the line connecting the two points. This allows the same method to generate rotational motion regardless of the size or shape of the object. This mechanism enables the sequential insertion of a spatula into the gap between the tilted objects and the tray floor, transportation with the object on the spatula, and the removal of the spatula.

III. Implementation of a Prototype

A. Method of the Gap-Generation Operation

Although the method shown in Fig. 4 is ideal in that it generates a large moment in the backward tilting motion, the method shown in Fig. 5 was devised and realized considering the ease of generating a trajectory of the contact area. By moving the body part straight to the left-hand side, a pushing force was applied from the top edge of the object to generate a moment for rotational motion. A linear guide was provided between the contact section and main body, and the contact section can slide up and down such that the contact section maintains the point of contact with the object even when the object rotates. In addition, a limit-switch was mounted on the body to prevent the object from overturning by excessive pushing. The system is configured such that the limit-switch senses slide-up of the contact region caused by tilting of the object, and the body stops the pushing process.

B. Basic Structure

The prototype is equipped with three linear guides at the points indicated in red in Fig. 6. Linear guide-A allows the passive upward sliding of the contact area, B allows the linear movement of the spatula, and C permits the linear movement of the pivot. Motor-1 at the rear of the machine corresponds to the spatula linear motion in linear guide-B, motor-2 switches the spatula between the flexible and stiff states, and motor-3 moves the pivot linearly via linear guide-C. Motor-2 is used to move the spatula in the direction of the pivot, while motor-3 is used to move the pivot.

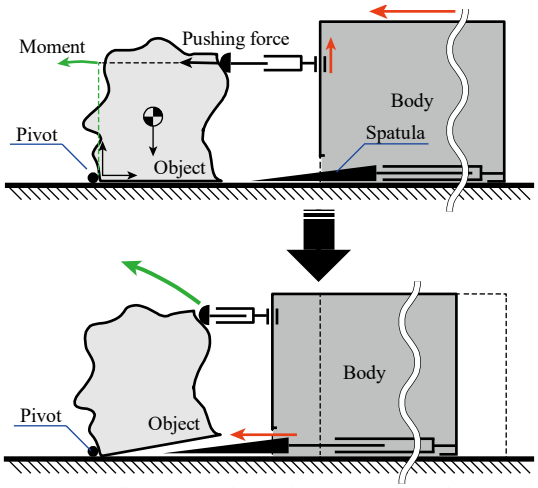

Figure 5. Configuration in the implementation of the backward-tilting gap-generation mechanism

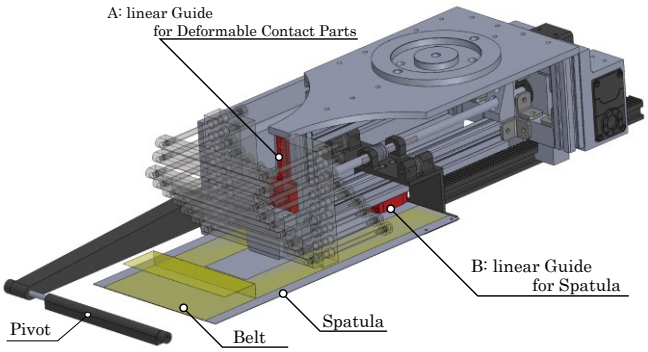

Figure 6. 3DCAD of the backward-tilting gap-generation mechanism

A tip-folding belt was wrapped around the spatula. This belt allowed the spatula to slide into an object without sliding friction. The belt mechanism is based on the principle of the "spatula mechanism for cell sheets", as described in Section 1-B (Fig. 1).

A notable feature of the contact region is that several parts that apply a pushing force to the object are mounted in parallel. The contact region is equipped with a spring in the shaft, so that when it is pressed against an object, the spring shrinks and the parts move to the right. By arranging several of these parts in parallel, each part sinks moderately, allowing a backward-tilting motion to occur in accordance with the shape of the object. This makes the mechanism versatile in terms of its ability to form complex shapes. The spatula must be as thin as possible to improve insertion while at the same time be sufficiently rigid to support a heavy load. Therefore, the thickness of the actual spatula was reduced to 0.3 mm, and a flexible-stiff switch function was installed to increase the stiffness of the spatula. This allows the spatula to hold up to 3 kg while improving its insertion.

The method for switching the stiffness of the spatula is described as follows. The center of the root side of the spatula was fixed to linear guide-B, as shown in Fig. 6. Two holes were drilled at each end of the root side of the spatula through which the ropes were threaded. A rope was wound around the pulley at the top of the spatula and secured. The shaft through the pulleys is rotated by motor-2 shown in Fig. 6, which tightens the rope and lifts both the ends of the spatula. This caused the spatula to bend. The bent spatula has a higher stiffness.

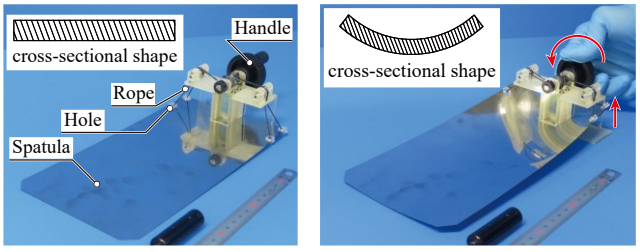

(a) Low Stiffness mode (b) High Stiffness mode

Figure 7. Stiffness changing of spatula

The actual switching of the spatula from flexible to stiff is illustrated in Fig. 7. Instead of utilizing motor-2, the pulley is rotated with the shaft by turning the handle. This tightens the rope and bends the spatula, resulting in a high stiffness.

C. Realization of a Prototype

A prototype was fabricated based on the configuration described in Section 2-B. The overall view is shown in Fig. 8, and Fig. 9 shows the prototype from three different angles. Table 1 lists the specifications.

The prototype was designed to be mounted as an end-effector on the robot arm "Universal Robot 3e" (here in after referred to as UR3e), one of the most widely used research manipulators, and because the maximum allowable load of UR3e was 3 kg, the sum of the mass of the prototype and objects was set to be less than 3 kg in this study. Fig. 2 shows the prototype operation as an end-effector of the UR3e robot arm. By mounting the prototype on the robot arm, the pushing motion can be outsourced to the robotic arm and does not need to be a part of the prototype itself. Therefore, the actuator to realize to pushing motion can be omitted, which reduces the requirements in terms of degrees of freedom, leading to a reduction in weight (approximately 2 kg, as shown in Table 1, top left part of Fig. 9). The maximum size of the object was arbitrarily set to 100 mm (length) × 100 mm (width) × 100 mm (height), and its maximum weight to 1 kg, so that the entire construct would be < 3 kg as mentioned above.

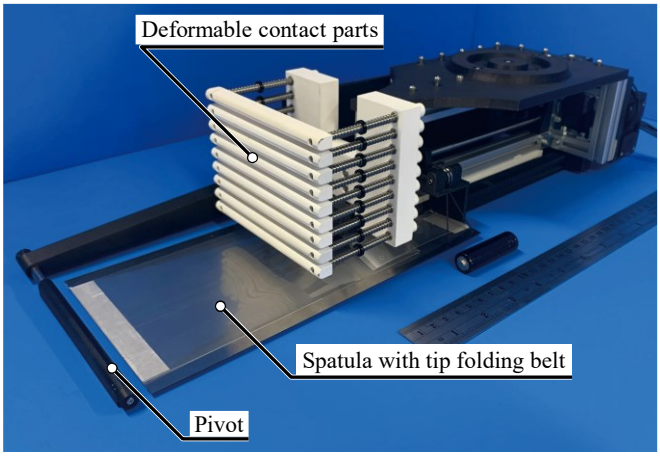

Figure 8. General view of the prototype

Table 1 Specifications

Dimentions	150×460×100 mm
Mass	1980g
Material of spatula	SUS304H
Size of spatula	120×240×0.3 mm

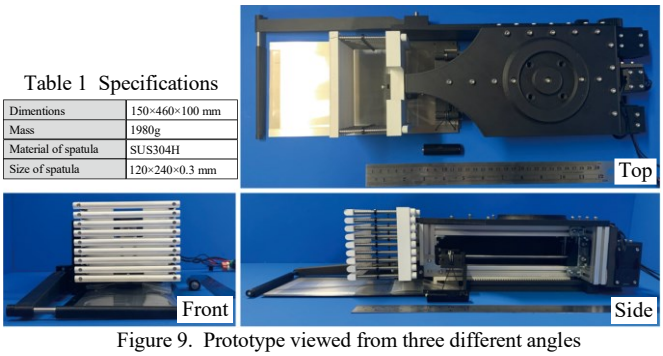

Figure 9. Prototype viewed from three different angles

D. Operation of the Prototype

The prototype performs scooping in the following three ways, depending on the shapes and properties of the object.

(a) Insertion of the spatula by tilting the object with a backward-tilting motion.

(b) Insertion of the spatula using a linear motion without a backward-tilting motion.

(c) Insertion of the spatula without a backward-tilting motion, using the spatula's linear motion and support of the pivot.

The objects to be scooped in each mode are:

(a) Objects with a complex shape whose bottom surface is completely in contact with the floor.

(b) Objects larger than the set size (100 × 100 mm).

(c) An object with a low height that is difficult to tilt using a backward-tilting motion.

Fig. 10 illustrates the flow of the trophy scooping operation in Mode-A.

(1) The end-effector is brought close to the object such that the spatula and pivot are clamped between them.

(2) The position of the pivot is fixed and the contact area is moved toward the pivot to tilt the object. The limit-switch senses tilting of the object and the end-effector stops pushing.

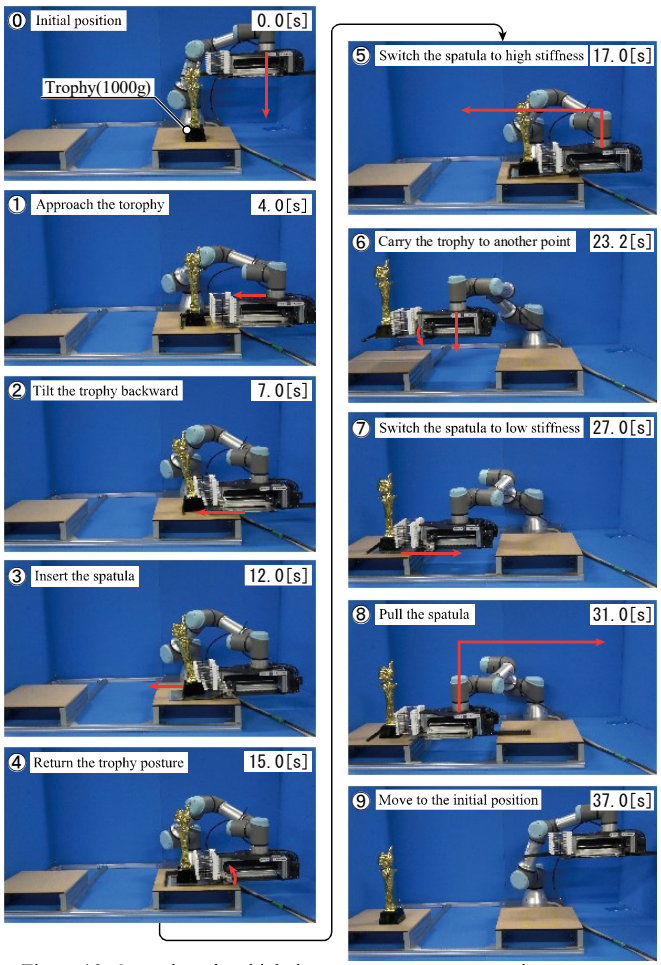

Figure 10. Operation via which the prototype scoops up and transports an object

(3) The spatula is inserted into the created gap.

(4) The distance between the pivot and contact area is increased to correct the inclination of the object.

(5) The spatula is bent to change from a low-stiffness state to a high stiffness state.

(6) The object is lifted and transported to another location.

(7) The curvature of the spatula is released and switched from stiff to flexible.

(8) The spatula is pulled out and the object is lowered.

(9) The end-effector is moved back to the initial position.

The above process is the sequence of operations in Mode-A. In Mode-B, the pivot is retracted to the contact side in case (1). In Mode-B and Mode-C, the operations in (2) and (4) are omitted, the spatula is sloped at an angle, and the bottom of the spatula is inserted along the bottom surface.

IV. Experiments with the Prototype

A. Comparison of the Soft and Stiff Modes

Experiments using a load-testing machine were conducted to evaluate the flexibility of the spatula in the low-stiffness mode and the load-carrying capacity of the spatula in the high-stiffness mode.

The experimental method is described as follows. Fig. 11(a) shows the experimental setup. For simplicity, the spatula mechanism was not equipped with a tip-folding belt. A tensile-testing machine was used to apply a downward displacement of 20 mm to a point 50 mm from the thin plate tip. The force applied to the given displacement was measured in both low- and high-stiffness modes.

The results are shown in Fig. 11(b). In the low-stiffness mode, a load of 0.57 N was applied for a displacement of 20 mm. This result confirmed the sufficient flexibility of the low-stiffness mode. In the high-stiffness mode, a load of 35.2 N was applied for a displacement of 20 mm. As the spatula did not buckle during the push-in process, the mechanism could support a target mass of 3 kg.

In contrast, for a load of 3 kg (29.4 N), the spatula was considered to have descended by 16.4 mm. A 5.9° inclination of the spatula makes it difficult to carry an object with a slippery bottom surface on the spatula. This may be overcome by optimizing the components of the spatula. Specifically, it is necessary to strengthen the rigidity of the parts that hold the spatula in place and to consider the optimal position of the hole through which the rope is threaded to bend the spatula, as well as the strength of the accompanying rope.

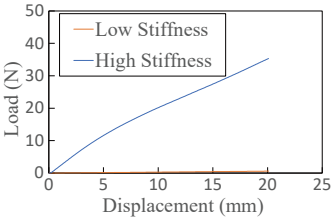

(a) Spatula load-testing method (b) Results of the spatula load tests

Figure 11. Comparison of the flexible and rigid modes by the spatula load test

B. Scooping Up Multiple Types of Objects

A scooping up experiment was conducted on multiple types of objects using the prototype. The integrated machine was mounted as an end-effector of UR3e as shown in Section 3-D, and the three operation modes used in the experiment were executed for all patterns on each prepared object. A correct or incorrect scooping up process was determined for each pattern. Success was defined as three out of three successful scoopings.

The results are shown in Fig. 12. The photographs were classified into those operated in Mode-A and those operated in Modes-B and C. The first step is to insert the spatula into the gap.

First, an object with a gap to insert the spatula and a height that could be held in all modes was considered. Objects that can be held in Modes-A and C are those that have no gap to insert the spatula but can be manipulated with the support of the pivot. An object that can be held only in Mode-A is a heavy object that has no space for the spatula to be inserted and cannot be manipulated with the spatula.

Fig 12. Scooping and carrying of multiple types of objects.

Objects that can be held in Mode-B and Mode-C are short objects that are difficult to tilt backward and possess curved and slippery contact surfaces, such as a PC mouse, as well as objects that should not be subjected to a pressing force, such as a crepe. An SD card case that can be held only by Mode-C is short, has a shape with no gap for inserting a spatula, and is lightweight. A block of tissue paper, which can be held only by Mode-B, is an exceptional case in which the object is larger than the expected size (100 × 100 mm) but flexible, and therefore it can be held by retracting the pivot and lifting the width restriction of the proposed system.

As described above, the prototype succeeded in scooping a wide variety of objects, including flexible objects for which the pressing force should not be applied, heavy objects, short objects, and objects with a bottom surface that is completely in contact with the ground surface with no space for the spatula to be inserted. This may be the result of the integration of the tip-folding belt, flexible and stiff switching modes of the spatula, and backward-tilting function, which expanded the range of objects that can be scooped-up and held.

V. Modeling and Validation of the Backward-Tilting Process

A. Objects that are Difficult to Scoop with the Prototype

There are some objects that may not be grasped in all modes. Examples are objects that are too short to be tilted backwards as shown in Fig. 13(a), as well as objects with no space for the spatula to be inserted, especially those with an extended hem with a concave skirt (Fig.13(a)), and objects with convex slope where the contact parts may slip upwards as shown in Fig. 13(b). To develop countermeasures against objects such as that shown in Fig. 13(b), an object was modeled in terms of its mass, shape, and friction (see B).

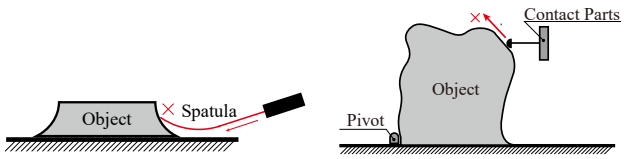

(a) Pseudosphere type object (b) Slippery object

Figure 13. Examples of objects that are difficult to scoop-up using the prototype

B. Tilt Angle of the Object required to Achieve Backward-Tilting

First, we considered the backward-tilting motion using a cube model. A sufficient amount of space is necessary to insert a spatula to achieve a backward tilt. Assuming that the length of one side of the cube is L=20 to100 mm and the tilt angle of the object is θ [°], the size of gap t can be expressed as $t=L\sin\theta$. When the gap size is t=1.0 mm (thickness of the spatula and belt = 0.4mm + a margin of 0.6mm), the relationship between L and θ is shown in the graph in Fig. 14. This graph shows that θ = 2.87° for L = 20 mm and θ = 0.573° for L = 100 mm. Therefore, the range of the tilt angle θ was set to θ = 0° to 2.87°.

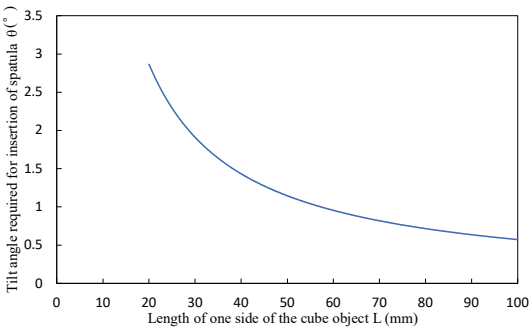

Figure 14. Relationship between the object size and tilt angle required for spatula insertion

C. Derivation of Conditions for Successful Backward-Tilting

The conditions for the backward tilt of an inclined object (as shown in Fig. 13(b)) are that the contact area tilts the object, and the contact area does not slide up the side of the object. The mechanical model diagram of tilting an object is shown in Fig. 15, assuming that the contact area and object are integrated at the moment of tilting. If the pushing force is F [N], mass of the object is M [kg], mass of the contact area is m [kg], and coefficient of friction between the object and the ground is μ_G, the conditions for the object to tilt are:

$$F > \frac{Mgx + mgX + \mu_G(M+m)gy_G}{y}, \quad (1)$$

where x, X, and y are values that vary with θ. When the height of the contact point between the object and contact zone is set at the highest point minus 10 mm, x, X, and y are expressed as follows:

$$x = \frac{L}{\sqrt{2}}\cos\left(\theta + \frac{\pi}{4}\right) + y_G tan\theta, \quad (2)$$

$$X = \sqrt{2L^2 - 20L + 100}\cos\left\{\theta + \frac{\pi}{4} - cos^{-1}\left(\frac{L-5}{\sqrt{L^2 - 10L + 50}}\right)\right\} + y_G tan\theta, \quad (3)$$

$$y = \sqrt{2L^2 - 20L + 100}\sin\left\{\theta + \frac{\pi}{4} - cos^{-1}\left(\frac{L-5}{\sqrt{L^2 - 10L + 50}}\right)\right\} - y_G. \quad (4)$$

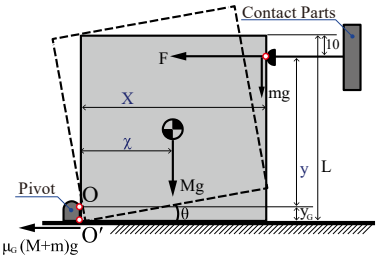

Figure 15. Mechanical model of object tilting

Next, we consider the conditions under which the contact area does not slide. Fig. 16 shows a mechanical model for pushing an object with an inclination. Assuming that the inclination angle of the object is Φ [°] and the coefficient of friction between the object and contact area is μ, the condition that the contact area does not slide up is expressed by the following equation:

$$F > \frac{\mu\sin(\theta+\varphi) + \cos(\theta+\varphi)}{\sin(\theta+\varphi) - \mu\cos(\theta+\varphi)}mg \quad (\sin(\theta+\varphi) - \mu\cos(\theta+\varphi) < 0), \quad (5)$$

$$F \le \frac{\mu\sin(\theta+\varphi) + \cos(\theta+\varphi)}{\sin(\theta+\varphi) - \mu\cos(\theta+\varphi)}mg \quad (\sin(\theta+\varphi) - \mu\cos(\theta+\varphi) > 0). \quad (6)$$

Equation (5) is omitted here because the right-hand side is negative and always holds true. Therefore, the condition for backward collapse is expressed by Equation (7).

$$\frac{Mgx + mgX + \mu_G(M+m)gy_G}{y} < F \le \frac{\mu\sin(\theta+\varphi) + \cos(\theta+\varphi)}{\sin(\theta+\varphi) - \mu\cos(\theta+\varphi)}mg. \quad (7)$$

When the parameters are set as M=1.0, m=0.14 kg, L=100 mm, μ_G=0.124, and θ=0.573°, Eq. (7) is represented by the graph in Fig. 17. The colored lines represent the friction coefficient μ between the object and contact area, varying from 0 to 2.0 in increments of 0.2. When μ is 0, the green area represents range in which the contact area tilts the object, and the red area represents range in which the contact area slides up the side of the object.

The above process enables us to theoretically determine the relationship between the friction coefficient μ of the object and the contact area and inclination angle Φ of the object for arbitrary parameters.

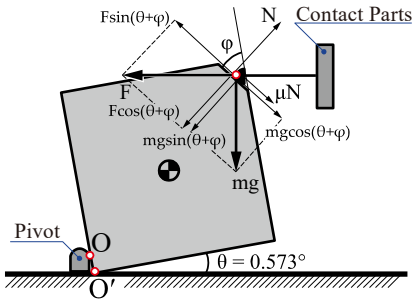

Figure 16. Mechanical model of the contact area sliding up the object

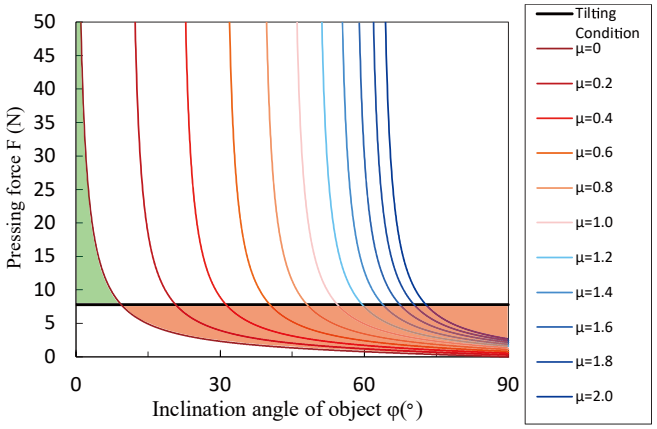

Figure 17. Region in which the contact area slides up the object considering the inclination angle Φ of the object and the pushing force F

D. Experiments to Verify the Validity of the Theoretical Model

D-1. Experimental Method

To evaluate the validity of the developed theoretical model, a push-in experiment was conducted using a prototype. First, the experimental apparatus shown in Fig. 18 converts the tensile force F of the tensile testing machine into the pressing force F at the contact area for measurement according to the following procedure. The object and pivot are placed on a foundation assembled with an aluminum frame. The prototype

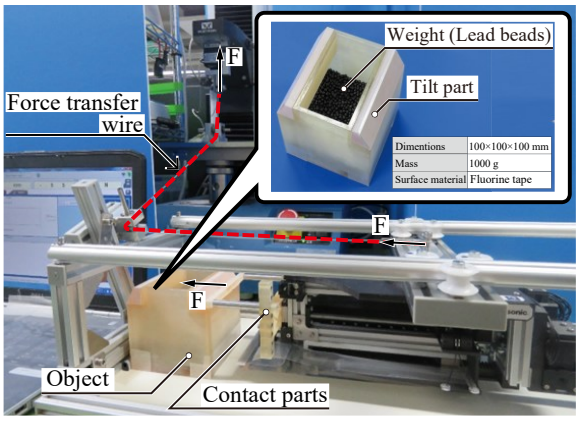

Figure 18. Device for backward-tilting experiments

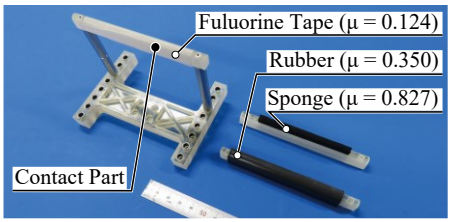

Figure 19. Three types of contact parts (μ is the value obtained when the contact region includes fluorine tape)

is suspended from the top, and the green frame and rollers allow smooth linear movement. When the tensile tester is driven upward, the prototype moves linearly to the left in Fig. 19 through the wire. This linear motion causes the contact area to generate a force F that is pressed against the object. In this experiment, the wire is pulled to 20 mm and the generated force F is measured. The object consists of a region whose mass M can be varied and an inclined part whose inclination angle Φ can be changed from 0° to 80° in 10° increments. The surface of the inclined region is covered with fluorine tape to determine the coefficient of friction. Three different surface materials are used as contact parts. By pressing these parts into the object, the relationship between the friction coefficient μ of the object, contact region, and inclination angle Φ of the object was measured.

D-2. Experimental Results

The measurement results are shown in Table 2 and Figs. 20(a) to 20(c). The maximum push-in force is plotted in green, and the push-in force when the object tilts or the contact area slides up is plotted in blue.

The results are approximately correct because they show the trends of the theoretical model. In Table 2, a green box with a checkmark indicates a successful backward tilt and a red box with a cross indicates a failed backward tilt. The yellow boxes with triangles indicate that the contact area slid up, but the object tilted slightly, which is a mixture of these two states.

The results for Φ = 40° and 50°, as shown in Fig. 20(b), are considered. Theoretically, once sufficient force is applied for the contact point to slide up the object, the object will continue to slide up without the need for further pushing force. However, the values of the green points in Fig. 20(b) exceeded those of

Table 2 Results of the backward-tilting experiment

φ \ μ	0.124 Fluorine tape	0.350 Rubber	0.827 Sponge
0°	✓	✓	✓
10°	✓	✓	✓
20°	✓	✓	✓
30°	×	✓	✓
40°	×	△	✓
50°	×	△	✓
60°	×	×	×
70°	×	×	×
80°	×	×	×

✓ : Successful backward-tilting (Contact area tilts the object)
× : Failure backward-tilting (Contact area slides up)
△ : The contact area slides up, but it tilts the object slightly

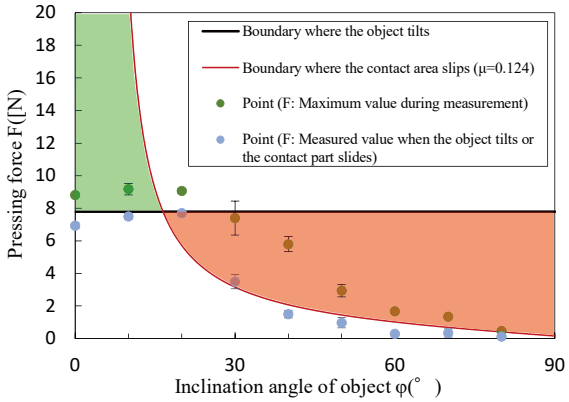

(a) Surface of the contact part: fluorine tape

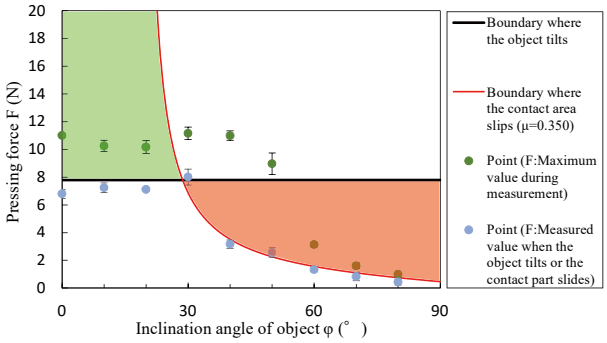

(b) Surface of the contact part: rubber

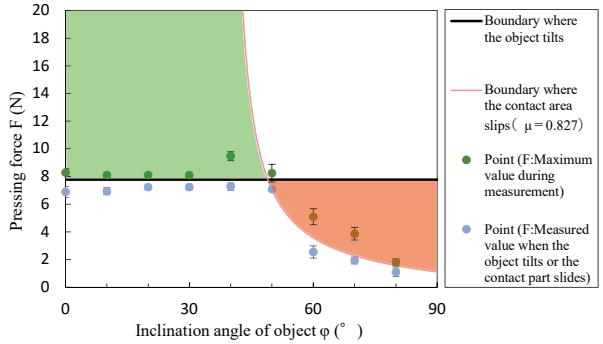

(c) Surface of the contact part: sponge

Figure 20. Backward-tilting experimental results obtained when the object surface was fluorine tape

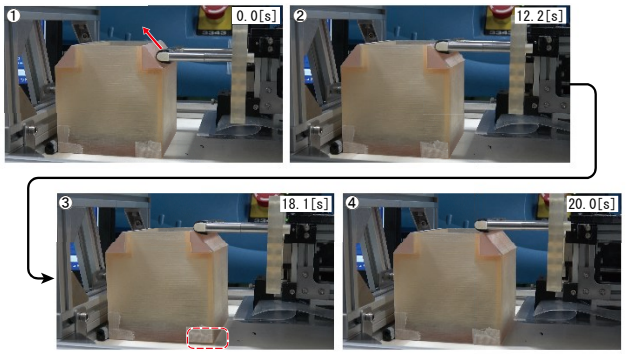

Figure 21. Experimental behavior of the backward-tilting process at Φ = 40° between the object (fluorine-tape surface) and contact area (rubber-sheet surface) .The red dotted frame in the figure shows the generation of a gap.

the blue points in all measurements. The two points at Φ = 40° and 50° shown in Fig. 20(b), where the green point is higher than the black line while the system undergoes slipping, are expected to exhibit a mixture of inclination and slipping, as indicated in Fig.21.

The high maximum values that were measured here may have resulted from slight undulations on the surface of the contacted material, which caused a higher friction force as the contact area slid.

In this section, we use a cubic model to derive the relationship between the coefficient of friction and inclination angle of the object to which the contact area slides. This model may be improved to be applicable to objects with complex shapes.

VI. CONCLUSION

The purpose of this study was to realize an end-effector that can scoop-up and transport a wide variety of objects uniformly by focusing on a large setup and changeover time, which is an issue in high mix, low-volume production systems. We developed the principle of an end-effector that integrates three important technological elements to realize these requirements: the "tip folding belt mechanism," "cross-sectional, quadratic-moment flexible/stiff-switching mechanism," and the "backward-tilting mechanism for creating a gap for inserting a spatula. " Using the prototype, we conducted experiments to scoop-up and transport a wide variety of objects and achieved the scooping-up and transport of these objects. The prototype was applicable to high-mix low-volume production systems. Based on the results of the loading test involving the spatula and the modeling of objects that can be tilted backwards, we plan to further improve the scooping performance of the mechanism and expand its field of activity by increasing the size of this system. In addition, the current backward-tilting model may be improved such that it can be applied to objects with complex shapes.

REFERENCES

[1] G. Hirzinger et al., “A mechatronics approach to the design of light-weight arms and multifingered hands,” in Proc. 2000 ICRA. Millenn. Conf. IEEE Int. Conf. Robot. Autom. Symp. Proc. (Cat. No.00CH37065), 2000, vol. 1, no. April, pp. 46–54.

[2] J. Butterfass, M. Fischer, M. Grebenstein, S. Haidacher, and G. Hirzinger, “Design and experiences with DLR hand II” in Proc. World Autom. Congr. Proc. 10th Int. Symp. Robot. with Appl., pp. 105–109, 2004.

[3] W. Townsend, “The barretthand grasper – programmably flexible part handling and assembly,” Ind. Robot An Int. J., vol. 27, no. 3, pp. 181–188, Jun. 2000.

[4] Barret Technology Inc., “Barret hand BH8-282,” [Online]. Available: http: //www.barrett.com/robot/index.htm

[5] I. Gaiser et al., “A new anthropomorphic robotic hand,” inProc. - 8th IEEE-RAS Int. Conf. Humanoid Robots, 2008, no. August 2016, pp. 418–422.

[6] G. Grioli, M. Catalano, E. Silvestro, S. Tono, and A. Bicchi, “Adaptive synergies: An approach to the design of under-actuated robotic hands,” in Proc. IEEE Int. Conf. Intell. Robot. Syst., 2012, pp. 1251–1256.

[7] M. G. Catalano, G. Grioli, E. Farnioli, A. Serio, C. Piazza, and A. Bicchi, “Adaptive synergies for the design and control of the Pisa/IIT softhand,” Int. J. Rob. Res., vol. 33, no. 5, pp. 768–782, Apr. 2014.

[8] C. Piazza, C. D. Santina, M. Catalano, G. Grioli, M. Garabini, and A. Bicchi, “SoftHand pro-d: Matching dynamic content of natural user commands with hand embodiment for enhanced prosthesis control,” in 2016 IEEE Int. Conf. Robot. Automat. (ICRA), 2016, pp. 3516–3523.

[9] M. Tavakoli, and A. T. de Almeida, “Adaptive under-actuated anthropomorphic hand: ISR-SoftHand,” in Proc. IEEE/RSJ Int. Conf. Intell. Robots Syst., 2014, pp. 1629–1634.

[10] M. Tavakoli, R. Batista, and L. Sgrigna, “The UC softhand: Light weight adaptive bionic hand with a compact twisted string actuation system,” Actuators, vol. 5, no. 1, p. 1, Dec. 2015.

[11] H. Takeuchi, and T. Watanabe, “Development of a multi-fingered robot hand with softness-changeable skin mechanism,” in Proc. Joint 41st Int. Symp. Robot. 6th German Conf. Robot., 2010, vol. 1, pp. 606–612.

[12] Kenjiro Tadakuma, Nobuyuki Tanaka, Yuji Haraguchi, Mitsuru Higashimori, Makoto Kaneko, Tatsuya Shimizu, Masayuki Yamato, and Teruo Okano, "A device for the rapid transfer/transplantation of living cell sheets with the absence of cell damage," Biomaterials, Vol. 34, No. 36, pp. 9018-9025, Dec. 2013.

[13] T. Watanabe , K. Morino, Y. Asama, S. Nishitani, and R. Toshima, “Variable-Grasping-Mode Gripper With Different Finger Structures For Grasping Small-Sized Items”, IEEE Robotics and Automation Letters, vol. 6, no. 3, July 2021.

[14] T. Yoshimi, N. Iwata, M. Mizukawa, and Y. Ando, “Picking up operation of thin objects by robot arm with two-fingered parallel soft gripper,” in Proc. IEEE Workshop Adv. Robot. its Social Impacts, 2012, pp. 7–12.

[15] L. U. Odhner, R. R. Ma, and A. M. Dollar, “Open-loop precision grasping with underactuated hands inspired by a human manipulation strategy,” IEEE Trans. Autom. Sci. Eng., vol. 10, no. 3, pp. 625–633, Jul. 2013.

[16] L. U. Odhner et al., “A compliant, underactuated hand for robust manipulation,” Int. J. Rob. Res., vol. 33, no. 5, pp. 736–752, Apr. 2014.

[17] T. Ko, “A tendon-driven robot gripper with passively switchable underactuated surface and its physics simulation based parameter optimization,” IEEE Robot. Autom. Lett., vol. 5, no. 4, pp. 5002–5009, Oct. 2020.

[18] K. Morino, S. Kikuchi, S. Chikagawa,M. Izumi, and T.Watanabe, “Sheet-Based gripper featuring passive pull-in functionality for bin picking and for picking up thin flexible objects,” IEEE Robot. Autom. Lett., vol. 5, no. 2, pp. 2007–2014, 2020.